

Author Query Form

Journal: ARDP
Article: ARDP202000180

Dear Author,

During the copy-editing of your paper, the following queries arose.

Please refer to the query reference callout numbers in the page proofs and respond to each by marking the necessary comments using the PDF annotation tools.

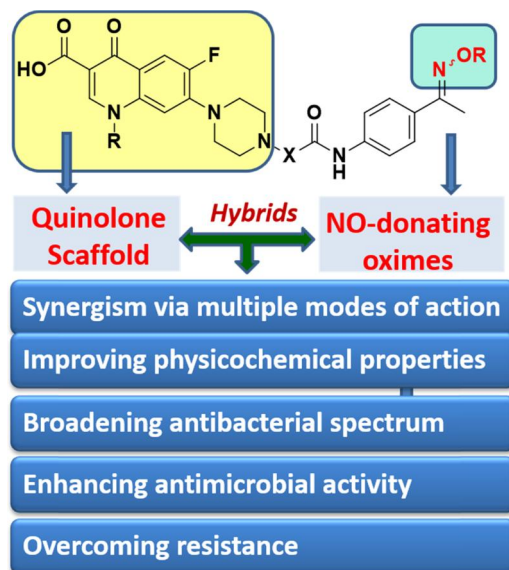
Please remember illegible or unclear comments and corrections may delay publication.

Many thanks for your assistance.

Query Reference	Query	Remarks/Comments	Query Reviewed
Q1	AUTHOR: Please confirm that given names (blue) and surnames/family names (vermillion) have been identified correctly.		
Q2	AUTHOR: Please verify that the linked ORCID identifiers are correct for each author.		
Q3	AUTHOR: Please provide significance for the bold values given in Table 1.		
Q4	AUTHOR: Please check whether the intended meaning of the sentence is retained after making the edits in the sentence beginning "Then, validation of the docking process was done by redocking..."		
Q5	AUTHOR: Please provide the month of accessing the website in Ref. [1].		

Graphical Abstract


The contents of this page will be used as part of the graphical abstract of html only. It will not be published as part of main.



A new series of nitric oxide-donating fluoroquinolone/oximes was prepared in this study. Evaluation of their antitubercular activity revealed that ketone derivatives **2b** and **2e** and oximes **3b** and **3d** exhibited somewhat higher activity than their respective parent fluoroquinolones. More important, oximes **3c–e** are highly potent against *Klebsiella pneumoniae*, whereas ketone **2c** and oxime **4c** are more active against *Staphylococcus aureus* than ciprofloxacin.

FULL PAPER

Synthesis and antimicrobial evaluation of new nitric oxide-donating fluoroquinolone/oxime hybrids

Hossameldin A. Aziz¹ | Gamal A. I. Moustafa¹ | Gamal El-Din A. Abuo-Rahma¹  | Safwat M. Rabea¹ | Glenn Hauk² | Siva K. Vagolu³ | Dharmarajan Sriram³ | James M. Berger² | Samar H. Abbas¹

¹Department of Medicinal Chemistry, Faculty of Pharmacy, Minia University, Minia, Egypt

²Department of Biophysics and Biophysical Chemistry, School of Medicine, John Hopkins University, Baltimore, Maryland

³Department of Pharmacy, Birla Institute of Technology and Science, Pilani, Hyderabad Campus, Hyderabad, India

Correspondence

Gamal El-Din A. Abuo-Rahma, Department of Medicinal Chemistry, Faculty of Pharmacy, Minia University, Minia 61519, Egypt.
Email: gamal.aborahma@mu.edu.eg

Present address

Gamal A. I. Moustafa, Department of Chemistry, University of Southampton, Southampton, UK.

Abstract

A new series of nitric oxide-donating fluoroquinolone/oximes was prepared in this study. The nitric oxide release from the prepared compounds was measured using a modified Griess colorimetric method. The antitubercular evaluation of the synthesized compounds indicated that ketone derivatives **2b** and **2e** and oximes **3b** and **3d** exhibited somewhat higher activity than their respective parent fluoroquinolones. Mycobacterial DNA cleavage studies and molecular modeling of *Mycobacterium tuberculosis* DNA gyrase were pursued to explain the observed bioactivity. More important, antibacterial evaluation showed that oximes **3c–e** are highly potent against *Klebsiella pneumoniae*, with minimum inhibitory concentration (MIC) values of 0.06, 0.08, and 0.034 μM , respectively, whereas ketone **2c** and oxime **4c** are more active against *Staphylococcus aureus* than ciprofloxacin (MIC values: 0.7, 0.38, and 1.6 μM , respectively). Notably, the antipseudomonal activities of compounds **2a** and **4c** were much higher than those of their respective parent fluoroquinolones.

KEYWORDS

antibacterial, antitubercular, cleavable DNA complex, fluoroquinolones, nitric oxide

1 | INTRODUCTION

Tuberculosis is an infectious disease caused by the bacillus *Mycobacterium tuberculosis* (MTB).^[1] It is considered one of the top 10 causes of deaths globally; approximately 1.7 billion people were infected with latent *M. tuberculosis* worldwide, according to 2019 WHO report, who are, thus, at the risk of developing active tuberculosis disease during their lifetime.^[1] The widespread increase of multidrug-resistant TB (MDR-TB), extensively drug-resistant TB (XDR-TB), and totally drug-resistant TB (TDR-TB) is another serious concern that poses a huge financial burden on a global level. In addition, the current long-term TB treatment regimens using expensive and toxic drugs continue, for obvious economic and safety issues, to complicate the worldwide control of TB.^[2] The eradication of resistant tuberculosis requires treatment for up to 2 years in some cases and unfortunately, death is the end of many cases of drug-resistant

tuberculosis.^[3] Therefore, there is an urgent need to develop novel anti-TB agents with a shorter treatment duration, which, at the same time, are more active against MTB in both active and latent phases.^[4]

DNA gyrase is an ATP-dependent enzyme that plays a crucial role in all bacteria. It is necessary for the transcription, replication of DNA, and chromosome segregation processes. Therefore, DNA gyrase has been a classical target for the evolution of new antibacterial agents.^[5] The only DNA gyrase and/or topoisomerase IV inhibitors used in clinical practice as antibacterial agents are fluoroquinolones.^[5] The unique mechanism of quinolones provides a broad antibacterial spectrum benefit for their use over other antibiotics, because the DNA replication process is universal to all bacteria.^[6] Fluoroquinolones are, thus, active against a wide spectrum of aerobic Gram-positive organisms such as staphylococci, *Streptococcus pneumoniae*, *Enterococcus faecalis*, and *Nocardia* species, as well as Gram-negative organisms like *Haemophilus influenzae*, *Neisseria*

meningitides and *N. gonorrhoeae*, and *Pseudomonas aeruginosa*.^[7,8] Moreover, fluoroquinolones have an excellent safety profile and appropriate pharmacokinetic properties.^[6,7] Among the second-line fluoroquinolones approved for the treatment of tuberculosis by WHO are ciprofloxacin, ofloxacin, and levofloxacin.^[9] However, their therapeutic use was associated with the appearance of more dangerous and resistant strains of bacteria as a result of their misuse.^[7] This poses a significant challenge all over the world today to discover newer derivatives of fluoroquinolones to fight such resistance.

Nitric oxide (NO) is established as an important mediator formed by macrophages during bacterial infections, which have a critical role to eradicate the causative pathogens. Additionally, it can disrupt bacterial DNA, proteins, and signaling mediators, and interfere with macrophage apoptosis pathways.^[10] For instance, a significant antimicrobial effect of NO on the uropathogenic *Escherichia coli* isolates has been demonstrated. The host defense function in salmonella infections was also reported to be boosted by NO. Moreover, it was reported that the antimycobacterial activity of the known first-line isoniazid (INH) is directly attributed to the released NO during INH activation by the catalase-peroxidase KatG.^[11] It has also been proved that NO has an antibiofilm activity and renders the biofilm cells susceptible to antibiotics.^[12–14] Therefore, NO has received great attention to confront biofilm-associated bacterial infections.^[13] As such, many approaches to develop new anti-TB agents via hybridization of TB drugs with NO-releasing moieties were developed (Figure 1).^[15–20]

Given the aforementioned reports, we herein examine the impact of introducing the NO-donating oxime moieties on the antimicrobial potential of selected fluoroquinolones. The design includes

the synthesis of a new series of *N*-4-piperazinyl quinolone oxime derivatives, in which the unsubstituted or *O*-methyl-substituted oxime moieties are linked by an arylcarbamoylalkyl tether to the quinolone scaffold. The antibacterial activity of the new compounds against MTB and a range of Gram-positive and -negative bacteria were evaluated. The release of nitric oxide from the prepared compounds as well as mycobacterial DNA cleavage stimulation was measured. Molecular docking into the active site of MTB DNA gyrase was carried out to study the impact of the introduced substitutions at the piperazinyl *N*-4 nitrogen on the overall binding with DNA gyrase. In addition, we looked at the relationship between the antimycobacterial activity and the lipophilicity (cLogP) of the compounds, which is often a fundamental issue to consider in the quinolones' ability to penetrate the waxy cell wall of mycobacteria.

2 | RESULTS AND DISCUSSION

2.1 | Chemistry

2.1.1 | Synthesis of the target compounds 3a–f and 4a–f

The target compounds were synthesized as outlined in Scheme 1. Acylated derivatives of 4-aminoacetophenone **1a–b** were synthesized via reaction of *p*-aminoacetophenone with bromoacetyl bromide or 3-bromopropionyl chloride in dichloromethane in the presence of potassium carbonates.^[21,22] Preparation of compound **1c** was achieved through the addition of 4-aminoacetophenone to a mixed anhydride formed in situ via the treatment of 2-bromopropionic acid

COLOR FIG

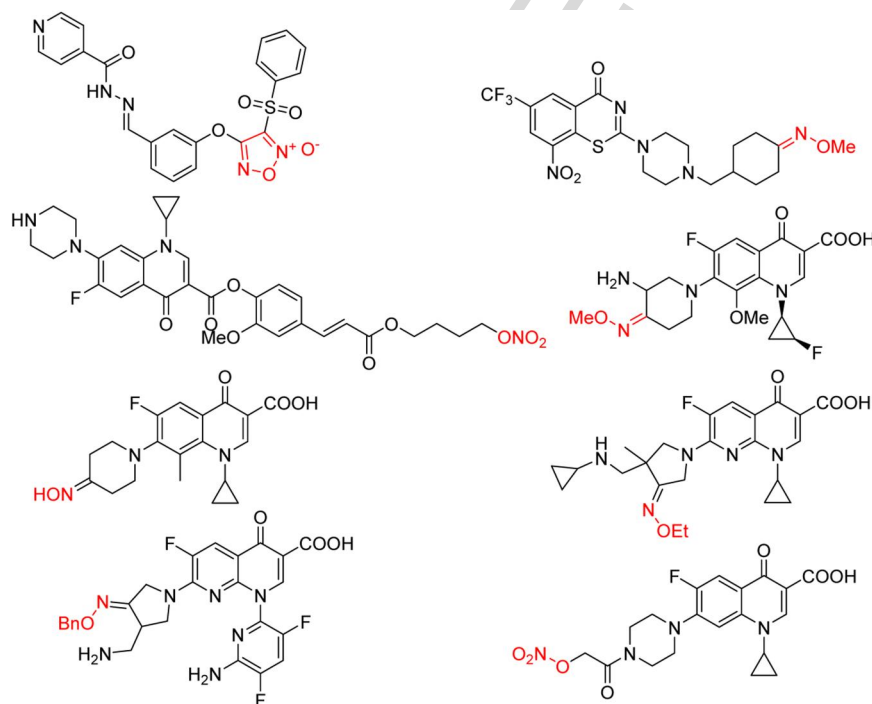


FIGURE 1 Examples of active antitubercular compounds containing NO-releasing moiety

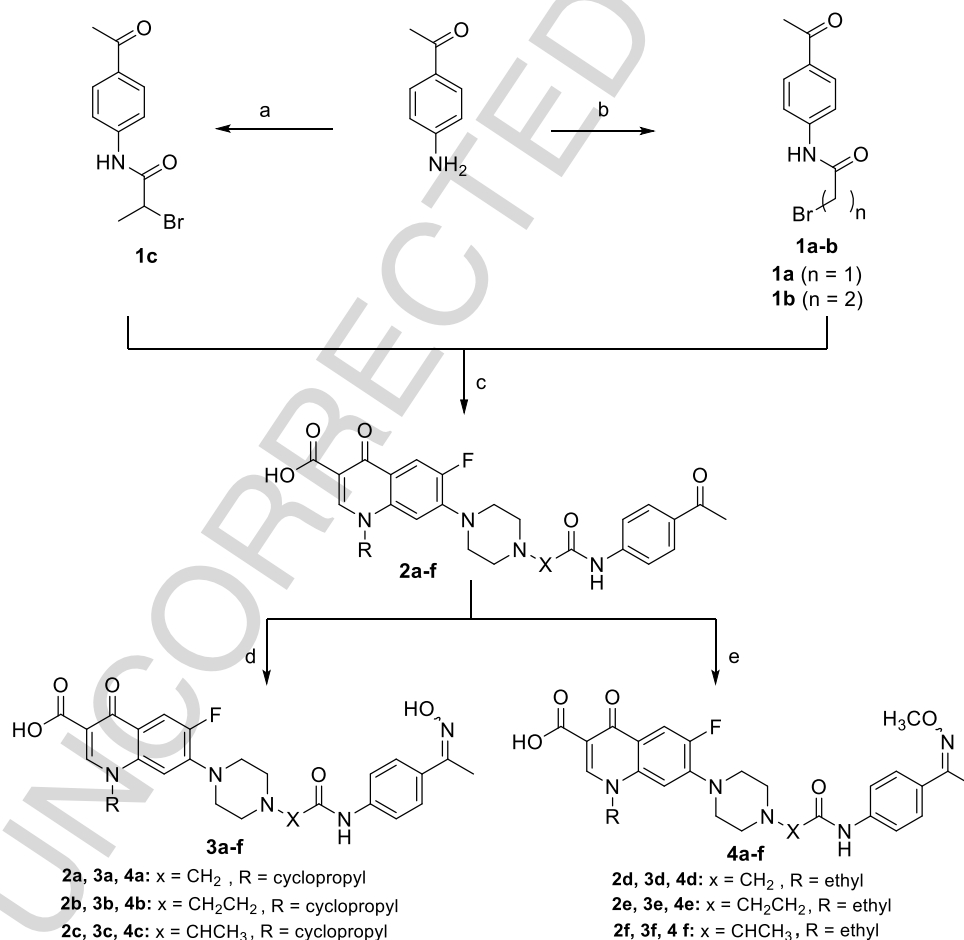
with ethyl chloroformate in the presence of triethylamine (TEA).^[23] Alkylation of ciprofloxacin or norfloxacin with haloamides **1a–c** was achieved in acetonitrile in the presence of TEA to afford ketones **2a–f**.^[21] The reaction of ketones **2a–f** with hydroxylamine hydrochloride or methoxyamine hydrochloride in ethanol afforded the target oximes **3a–f** and O-methyloximes **4a–f**, respectively.^[21,24] The synthesized compounds were characterized by infrared (IR), nuclear magnetic resonance (NMR), high-resolution mass spectrometry (HRMS), and elemental microanalyses.

The IR spectra of oximes **3a–f** showed the disappearance of ketonic carbonyl (COCH₃) due to its conversion to the ketoxime group (C=N–OH). ¹H-NMR spectra of compounds **3a–f** are characterized by the appearance of a new singlet signal at δ 10.91–10.96 ppm, assigned to OH of the oxime. The methyl protons in (CH₃C=N–OH) appeared to be upfield shifted by 0.38 ppm than the methyl of the precursor ketones due to the lower electronegativity of N than that of the O atom. ¹³C-NMR spectra of compounds **3a–f** showed the disappearance of the ketonic carbonyl (COCH₃) due to its conversion to the ketoxime group (CH₃C=N–OH), which appeared at δ 152.91–152.94 ppm. Furthermore, the carbon of (CH₃C=N–OH) appeared at δ 11.81–11.82 ppm, with a

significant upfield shift by a value of 15 ppm in comparison to the precursor (CH₃CO). However, ¹H-NMR spectra of compounds **4a–f** were characterized by the appearance of a new singlet signal at about δ 3.91–3.92 ppm, assigned to (CH₃C=N–OCH₃); the methyl protons of (CH₃C=N–OCH₃) appeared to be upfield shifted by 0.35 ppm than those of the precursor ketones. ¹³C-NMR spectra of compounds **4a–f** showed the disappearance of the ketonic carbonyl due to its conversion to (CH₃C=N–OCH₃), which appeared at δ 152.92–154.02 ppm, and the appearance of the O-methyl oxime carbon (CH₃C=N–OCH₃) at δ 61.91–61.97 ppm. Additionally, the methyl carbon of (CH₃C=N–OCH₃) appeared at δ 12.53–12.57 ppm, with an upfield shift by a value of ~14 ppm in comparison to the precursor (CH₃C=O).

2.1.2 | Measurement of nitric oxide release using a modified Griess method

NO release from the target oximes **3a–f** was measured by a modified Griess method.^[21] NO release from the tested compounds was measured at 100- μ M concentration and assessed in the stable nitrite curve, relative



SCHEME 1 The synthesis of the intermediates **2a–f**, oximes **3a–f**, and O-methyloximes **4a–f**. Reagents and conditions: (a) CH₃CH(Br)COOH, CICOEt, TEA, CH₂Cl₂; (b) BrC(O)CH₂Br/BrCH₂CH₂C(O)Cl, K₂CO₃, H₂O, CH₂Cl₂; (c) ciprofloxacin/norfloxacin, CH₃CN, Et₃N; (d) NH₂OH.HCl, EtOH; e: NH₂OCH₃.HCl, EtOH

to that of a standard sodium nitrite solution, and calculated as the amount of NO released (mol/mol) %. As shown in Table 1, some detectable amounts of NO in the range of 6%–9% (mol of NO/mol of the tested compound) were observed, albeit in much lower amounts than those obtained from the reference NaNO₂ (positive control), which could be basically explained by the solubility issues of the tested compounds in the aqueous buffer system. We have not tested the NO release from O-methyl oximes **4a–f**, as they normally require in vivo O-demethylation to the free oximes before NO release.

2.2 | Biological evaluation

2.2.1 | Evaluation of antimycobacterial activity

In vitro screening of against *M. tuberculosis*

The in vitro antimycobacterial activity for compounds **2a–f**, **3a–f**, and **4a–f** was evaluated against *M. tuberculosis* H37Rv strains. To study the effect of lipophilicity on the antitubercular activity, cLogP values of target compounds were calculated by ChemDraw Professional 15.1 (Table 2). The correlation coefficient between cLogP and biological activity against MTB H37Rv showed that the *R* value is 0.3988. Therefore, there is a slow correlation between calculated cLogP and the bioactivity, which means that the activity would only increase slightly if logP increases. This implies that lipophilicity is not the sole parameter affecting the biological activity.

As noticed in Table 2, ciprofloxacin ketone derivative **2b** and its corresponding oxime **3b** exhibited higher potency against *M. tuberculosis* H37Rv (MIC 1.5 μM) than ciprofloxacin (MIC 2.4 μM). Norfloxacin ketone derivative **2e** (MIC 3.1 μM) exhibited a threefold increase in the activity than norfloxacin (MIC 9.8 μM). Moreover, norfloxacin oxime derivative **3d** is more potent against *M. tuberculosis* H37Rv (MIC 6.2 μM) than norfloxacin (MIC = 9.8 μM). Despite their higher lipophilicity, O-methyl oxime derivatives **4a–f** showed lower potency than their parent compounds. Such reduction in the antimycobacterial activity revealed that lipophilicity of the molecule, and hence penetration into the mycobacteria, is not the sole factor that can affect the bioactivity. Indeed, other physicochemical parameters like electronic factors and molecular mass must be considered. Moreover, the structural changes should have an impact on the affinity of the compounds for their target DNA gyrase. Overall, the prepared ciprofloxacin derivatives are more potent than their corresponding norfloxacin derivatives. In other words, through a simple structure–activity relationship (SAR) analysis, we found that hybrids containing (–CH₂CH₂–) tethers were more active than those containing (–CH₂–) or (–CH(CH₃)–). Also, the replacement of unsubstituted oxime (C=N–OH) with O-methyl oximes (C=N–OMe) reduces the activity.

DNA cleavage assay

Fluoroquinolones act by inhibition of DNA gyrase, a heterotetrameric (GyrA2GyrB2) enzyme that transiently produces double-stranded DNA breaks as it negatively supercoils DNA.^[25] The break-resealing

process after the DNA strand passage is prevented by fluoroquinolones. This leads to the creation of persistent covalent enzyme–DNA adducts called cleaved complexes. The formed cleaved complex can sequentially cause disturbance in normal DNA replication, induction of DNA damage, and cell death mechanisms.^[20] An excellent acceptable indicator for fluoroquinolones inhibition of DNA gyrase is the in vitro cleavable DNA gyrase complex assay. The ability of the target compounds to form cleaved complexes was studied by measuring the formation of linear DNA from a starting supercoiled plasmid, and data were compared to that of ciprofloxacin. The inhibition of DNA supercoil relaxation and the promotion of DNA cleavage were monitored by running gels in the absence or presence of ethidium bromide (a DNA-intercalating agent). The addition of ethidium bromide results in positive supercoiling of closed circular DNA species. This permits readily resolution of relaxed DNA from nicked and linear species. Compounds **2a**, **2b**, **3b**, and **3c** were selected to investigate their ability to promote DNA cleavage by *M. tuberculosis* gyrase. All the tested compounds induced DNA cleavage and nicked DNA (at 50–500 μM concentration), as shown in Figure 2.

Results showed that although some of the new compounds have improved MICs against *M. tuberculosis* H37Rv as compared with the parent fluoroquinolones, none of the new compounds were superior to the parent fluoroquinolones in terms of DNA cleavage stimulation. Thus, the new compounds may have an additional growth inhibition effect that is distinct from gyrase poisoning. This may be due to the alteration of physicochemical properties and/or release of nitric oxide.

In vitro cytotoxicity screening

Compounds **2a–d**, **2f**, **3a–f**, **4a**, **4c**, **4d**, and **4f** were tested at a single concentration of 10 μM against 60 cancer cell lines at the National Cancer Institute. All tested compounds showed no significant cytotoxic activity against tested cell lines (see Supporting Information Data), which is an indication of a selective antimicrobial activity with minimal toxicity to the mammalian cells.

2.3 | Docking studies

The most potent compounds, **2b**, **2e**, and **3b**, and the least potent compound, **4b**, were docked on topoisomerase II (gyrase) (PDB: 5bs8)

TABLE 1 The amount of NO released from compounds **3a–f** in a phosphate buffer of pH 7.4 (*n* = 3)

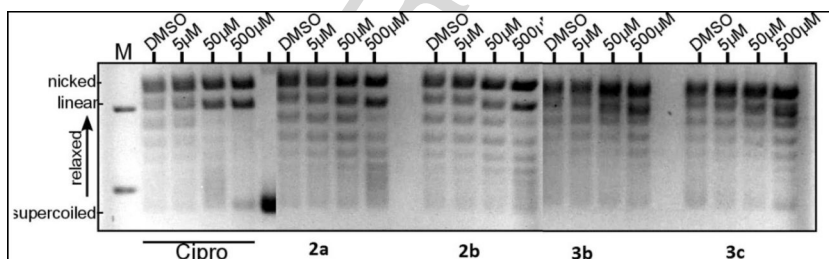
Compound	Amount of NO released % (mol/mol)
3a	6.78 ± 0.02
3b	7.76 ± 0.01
3c	6.39 ± 0.00
3d	8.34 ± 0.03
3e	9.09 ± 0.02
3f	5.92 ± 0.04
NaNO ₂	77.61 ± 0.03

Q3

TABLE 2 The minimum inhibitory concentration (MIC) values of the tested compounds against *Mycobacterium tuberculosis* (μM) and their cLogP values

Compound	MIC against <i>M. tuberculosis</i> (μM)	cLogP	Compound	MIC against <i>M. tuberculosis</i> (μM)	cLogP
2a	6.2	0.883	2d	12.7	0.764
2b	1.5	1.078	2e	3.1	0.943
2c	6	1.192	2f	12.3	1.073
3a	6	1.180	3d	6.2	1.060
3b	1.5	1.375	3e	47.9	1.240
3c	5.9	1.489	3f	12	1.709
4a	5.9	1.520	4d	48	1.400
4b	48	1.715	4e	48	1.580
4c	22.9	1.829	4f	46.7	1.709
Ciprofloxacin	2.4	-0.725	Norfloxacin	9.8	-0.780

FIGURE 2 DNA cleavage by *Mycobacterium tuberculosis* gyrase induced by ciprofloxacin, 2a, 2b, 3b, and 3c



to explore the possible binding interactions, imposed by the new structural modifications, on the active site of gyrase. Docking experiments were carried out using MOE 2014 software. The quality of the PDB file was examined by the *R* value. *R* is a measure of error between the observed intensities from the diffraction pattern and the predicted intensities that are calculated from the model, where *R* values of 0.20 or less make the model valid.^[26,27] The X-ray crystallographic structure of the ligand-enzyme complex was downloaded from protein data bank (www.rcsb.org); Topoisomerase II (gyrase) (PDB: 5bs8).^[28] The enzyme was prepared for docking process by automatic protein correction and adding hydrogens to the three-dimensional (3D) structure of protein. Then, validation of the docking process was done by redocking of the cocrystallized ligand, and RMS (root mean square) distance with MMFF94X force field, and the partial charges were automatically calculated. Then, the designed compounds were docked in a similar manner. Docking was carried out with the default settings of MOE-DOCK. The binding free energies from the major docked poses are listed in Table 3.

2.3.1 | Binding modes of tested compounds with topoisomerase II enzyme active site

The docking results indicated that all of the tested compounds appear to have an affinity for the enzyme, with binding free energy (ΔG) values ranging from -21.58 to -31.27 Kcal/mol, which is comparable

to moxifloxacin ($\Delta G = -25.13$ kcal/mol) and ciprofloxacin ($\Delta G = -21.58$ kcal/mol; Table 3).

The binding-score energies have negative values, suggesting that the binding of quinolone derivatives to the active site of the gyrase enzyme is spontaneous. Moreover, the docked compounds, parent quinolones (ciprofloxacin and norfloxacin), and the reference compound (moxifloxacin) form water-mediated chelation with magnesium ion through the C-3 carboxylic group and C-4 carbonyl functionality, hydrophobic interaction with the active site of the gyrase enzyme, hydrogen bonding with amino acid residue Arg128, water-mediated hydrogen bond with amino acid residues Asp C94 and Ser C91, and van der Waals interaction with

TABLE 3 ΔG values (Kcal/mol) of the tested compounds 2b, 2e, 3b, 4b, ciprofloxacin, norfloxacin, and moxifloxacin

Compound	ΔG values (kcal/mol)
Moxifloxacin	-25.13
Ciprofloxacin	-21.58
Norfloxacin	-23.68
2b	-31.27
2e	-26.79
3b	-27.18
4b	-30.36

COLOR FIG

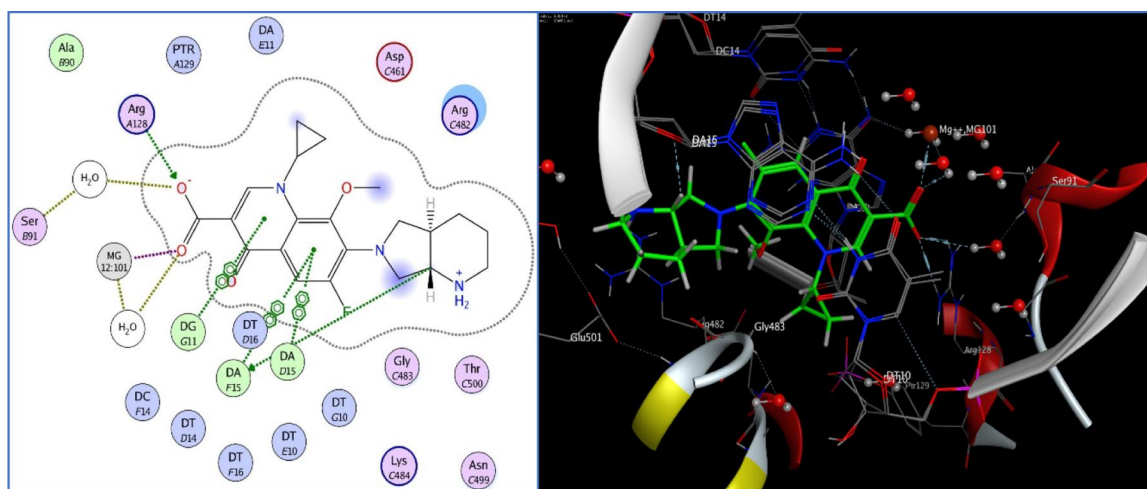


FIGURE 3 Two-dimensional and three-dimensional diagrams of moxifloxacin docked into the active site of *Mycobacterium tuberculosis* DNA gyrase

nucleotide bases through quinolone moiety or the introduced *N*-4 piperazinyl moiety (Figures 3–8). In addition, oxime derivative **3b** forms extra hydrogen bonding with gyrase nucleotide bases (e.g., DT H14 and DC F14), as shown in Figure 7. Despite the low binding free energy of *O*-methyl oxime **4b** ($\Delta G = -30.36$ kcal/mol), it displayed the weakest antimycobacterial activity. This lower potency may be attributed to other physicochemical parameters. In general, all the docked compounds did not exert additional significant bindings over the parent fluoroquinolones (ciprofloxacin, norfloxacin, and moxifloxacin), which is also supported by the in vitro DNA cleavable complex formation shown in Figure 2, thus again supporting the conclusion that the biological activity does not solely rely on additional binding to the active site, but also on the changes in physicochemical properties and/or donation of nitric oxide.

2.4 | Screening of antibacterial activities

The in vitro antibacterial activities of compounds **2a–f**, **3a–f**, and **4a–f** were evaluated against Gram-positive strains, *Staphylococcus aureus* (ATCC 6538), *Bacillus cereus* (AUMC No B-52), and *Micrococcus luteus* (AUMC No B-112), and against Gram-negative strains, *Klebsiella pneumoniae* (AUMC No B-77), *P. aeruginosa* (AUMC No B-73), *E. coli* (ATCC 8739), and *Serratia marcescens* (AUMC No B-54). The tested compounds were assayed in comparison to ciprofloxacin and norfloxacin as antibacterial references using the standard agar cup diffusion method^[29] and the MICs are shown in Table 4.

As shown in Table 4, ciprofloxacin derivatives **2a**, **2c**, and **4c** showed higher potency against *S. Aureus* as compared with the parent ciprofloxacin, with MICs of 3.4, 0.7, 0.38, and 1.4 μ M, respectively. Ketone **2c** and *O*-methyl oxime **4c** were more active than their

COLOR FIG

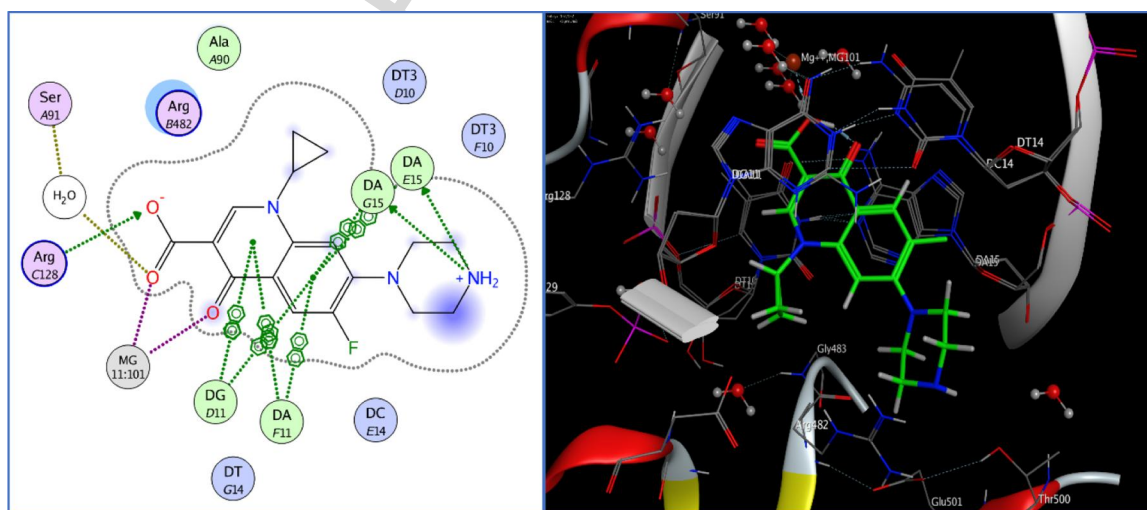


FIGURE 4 Two-dimensional and three-dimensional diagrams of ciprofloxacin docked into active site of *Mycobacterium tuberculosis* DNA gyrase

COLOR FIG

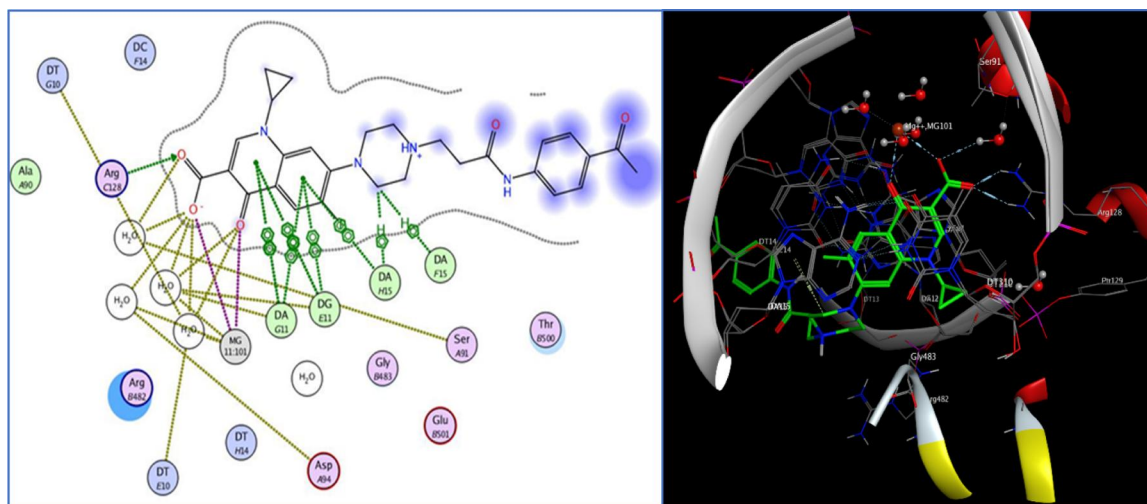
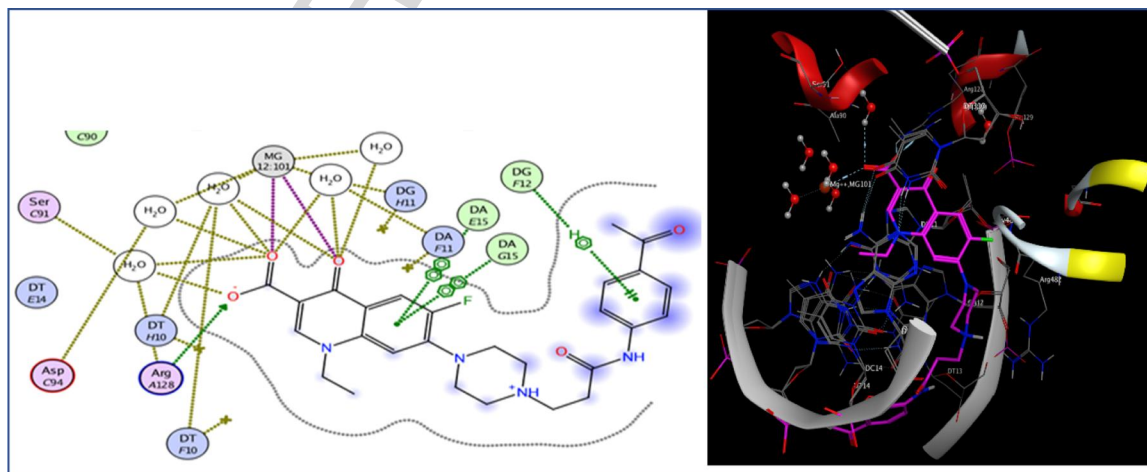


FIGURE 5 Two-dimensional and three-dimensional diagrams of compound 2b docked into the active site of *Mycobacterium tuberculosis* DNA gyrase

corresponding oxime **3c** against *S. aureus*. O-methyl oxime **4c** was four times more potent than ciprofloxacin against *S. aureus*. However, all the tested norfloxacin derivatives showed no pronounced activity against all the tested Gram-positive strains. Most of the tested compounds displayed a moderate-to-weak activity against *B. cereus* and *M. luteus*. The ciprofloxacin derivatives **2b**, **2c**, **3c**, and **4c** were highly active against *E. coli*, with MICs of 2.6, 1.1, 1.7, and 1.5 μM , respectively, whereas *E. coli* was resistant to all tested norfloxacin derivatives except **2f**, which exhibited a significant activity with an MIC value of 2.7 μM . In addition, it was found that compounds **2b** and **4b** displayed a potent activity against *S. marcescens*, with MICs of 17.7 and 5.5 μM , respectively. Meanwhile, compounds **2b**, **3c**, **3d**, and **3e** were highly potent against *K. pneumoniae*, with MICs of 1.4, 0.06, 0.08, and 0.034 μM , respectively. Notably, compounds **2b**, **2d**, and **4c** were more potent against *P. aeruginosa* as compared with ciprofloxacin with MICs of 1, 0.7, 0.2, and 1.6 μM , respectively.

Glancing at the abovementioned results, it was found that ciprofloxacin derivatives, in general, are more potent than the corresponding norfloxacin derivatives. It is worth mentioning that the N-(4-acetylphenyl)-2-(4-piperazinyl)propanamide moiety linked to the C-7 of quinolone ring generally enhanced the antibacterial activity against both Gram-positive and -negative bacteria. This observation is obvious in the following compounds: **2c**, which is highly active against *B. cereus* (MIC = 6.6 μM), **3c**, which exhibits a remarkable activity against *K. pneumoniae*, with MIC = 0.06 μM , and compound **4c**, which exhibited a potent activity against *S. aureus* and *P. aeruginosa*, with MICs of 0.38 and 0.2 μM , respectively. Additionally, it was found that oximation of the ketone intermediates resulted in enhancement of activity against *Kl. pneumoniae*, as seen with oximes **3c**, **3d**, and **3e**, which may arise from either improvement of physiochemical properties and/or the release of nitric oxide.

COLOR FIG



COLOR FIG

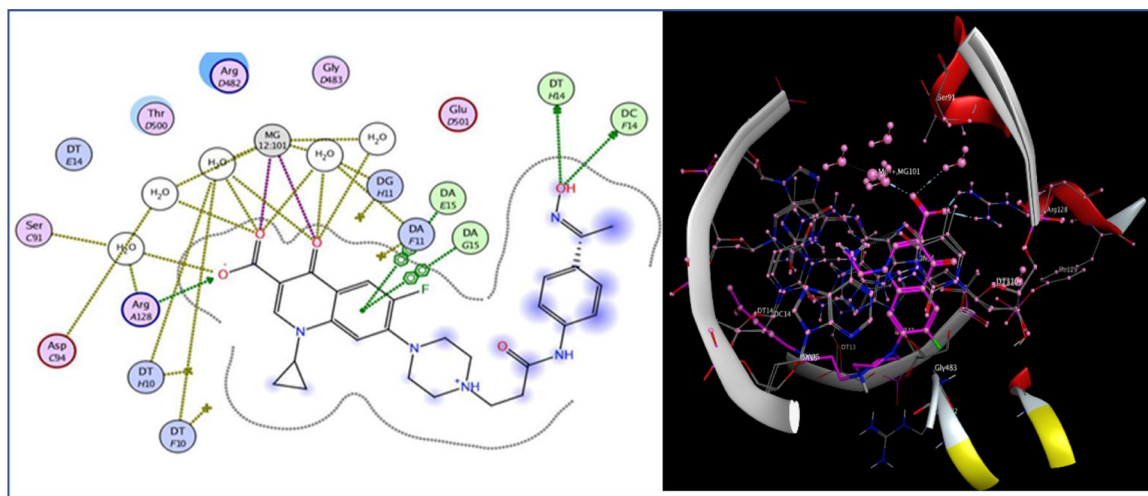


FIGURE 7 A two-dimensional diagram of compound **3b** docked into the active site of *Mycobacterium tuberculosis* DNA gyrase

3 | CONCLUSION

New nitric oxide-donating fluoroquinolones/oxime hybrids were synthesized and characterized by various spectroscopic techniques. In vitro antitubercular activity against *M. tuberculosis* H37Rv showed that the ketones and oxime derivatives of norfloxacin were generally lower than their parent fluoroquinolone. Inversely, ciprofloxacin analogs (the ketone derivatives **2b** and its corresponding oxime **3b**) showed an enhanced activity than the parent ciprofloxacin. The lack of systemic correlation between the MICs and clogP values of synthesized confirms the fact that the antimycobacterial activity is not only dependent on lipophilicity and penetration issues but also on different physiochemical parameters like electronic factors and molecular mass.^[28] The levels of cleaved DNA formed by the prepared compounds were lower than those of ciprofloxacin, which is not in agreement with the observed antimycobacterial activity. This potentially implies the existence of another mechanism besides DNA gyrase inhibition, such as NO release and/or improvement in cell wall penetration. Also, screening of antibacterial activity showed

that some of the tested compounds showed high potency against both Gram-positive and -negative bacteria than their parent fluoroquinolones, especially compounds having *N*-(4-acetylphenyl)-2-(4-piperazinyl) propanamide moiety linked to the C-7 of quinolone ring. More important, compounds **3c**, **3d**, and **3e** are highly active against *K. pneumonia* (MIC = 0.06, 0.08, and 0.034 μ M), whereas compounds **2a**, **2d**, and **4c** were highly potent against the clinically important *P. aeruginosa*, with MICs of 0.7, 1.0, and 0.2 μ M, respectively.

4 | EXPERIMENTAL

4.1 | Chemistry

4.1.1 | General

The reactions were monitored by thin-layer chromatography (TLC) using methylene chloride/methanol (19: 1 v/v). Melting points were

COLOR FIG

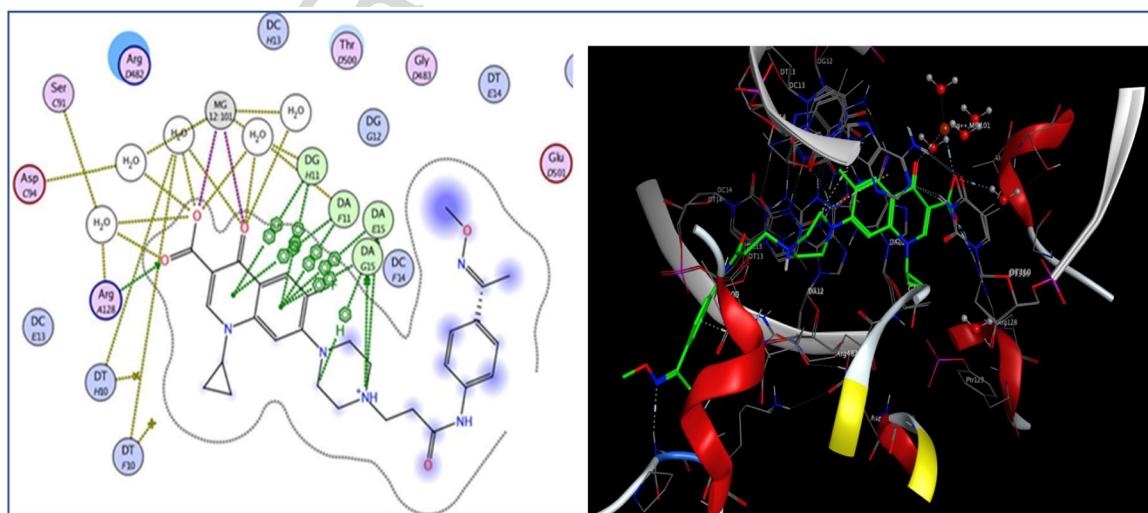


FIGURE 8 A two-dimensional diagram of compound **4b** docked into the active site of *Mycobacterium tuberculosis* DNA gyrase

TABLE 4 The minimum inhibitory concentration (MIC) values of the target compounds and their references ciprofloxacin and norfloxacin against the tested strains in (μM)

Compound	Bacterial strain						
	Gram-positive strains			Gram-negative strains			
	<i>Bacillus cereus</i>	<i>Staphylococcus aureus</i>	<i>Micrococcus luteus</i>	<i>Escherichia coli</i>	<i>Serratia marcescens</i>	<i>Klebsiella pneumonia</i>	<i>Pseudomonas aeruginosa</i>
2a	7.60	3.40	>50	>50	47.40	5.5	0.7
2b	9.60	>50	27	2.60	17.70	1.4	73.1
2c	6.60	0.70	>50	1.1	>50	6.6	25.40
2d	>50	>50	>50	>50	>50	>50	1
2e	>50	>50	>50	>50	>50	11.8	47.20
2f	>50	>50	>50	2.70	>50	>50	>50
3a	>50	>50	6.14	10.20	>50	>50	>50
3b	24.30	>50	>50	10.30	>50	>50	>50
3c	>50	>50	>50	7.8	>50	0.06	>50
3d	>50	>50	>50	>50	>50	0.08	>50
3e	>50	>50	>50	>50	>50	0.03	>50
3f	>50	>50	>50	>50	>50	3.50	>50
4a	>50	>50	>50	>50	>50	>50	>50
4b	>50	>50	32.60	>50	5.50	>50	>50
4c	>50	0.38	10	1.50	>50	>50	0.20
4d	>50	>50	>50	>50	>50	>50	>50
4e	>50	>50	>50	>50	>50	>50	>50
4f	>50	>50	>50	>50	>50	>50	>50
Ciprofloxacin	4.40	1.40	3.40	0.10	10	3.60	1.6
Norfloxacin	1.90	1.60	8.20	0.35	49.50	0.50	16

determined on an electrothermal melting point apparatus (Stuart Scientific Co.) and were uncorrected. IR spectra are recorded as KBr disks on a Shimadzu 408 instrument Spectrophotometer at the Faculty of Science, Sohag University. NMR spectra were measured on a Bruker AM NMR (400 MHz) spectrometer at the Faculty of Science, Sohag University. All numbers referring to NMR data obtained are expressed in parts per million (ppm). Elemental microanalyses for carbon, hydrogen, and nitrogen were performed at The Regional Center for Mycology and Biotechnology, Al-Azhar University, Cairo, Egypt. For TLC, the DC Alufolien, Kieselgel 60 F254 precoated plates were used (Merck, Darmstadt, Germany). HRMS spectra were collected via Thermo Scientific Q Exactive™ Orbitrap mass spectrometer and reported as mass/charge (m/z) with percent relative abundance at Faculty of Pharmaceutical Sciences, University of British Columbia, Vancouver Campus, Canada.

The InChI codes of the investigated compounds, together with some biological activity data, are provided as Supporting Information.

4.1.2 | General procedure for synthesis of compounds 1a–b^[21]

A potassium carbonate solution (0.690 g, 5 mmol) in water (30 ml) was added to a stirred solution of *p*-aminoacetophenone (0.675 g, 5 mmol) in DCM (30 ml) at 0–5°C. Then, bromoacetyl bromide (or 3-bromopropionyl chloride; 5.5 mmol) in DCM (30 ml) was slowly added over a period of 30 min. Stirring was continued for 2 hr at 0–5°C and then at room temperature for an additional 12 hr. The whole mixture was extracted with DCM (2 × 25 ml) and washed with water (2 × 25 ml). The combined organic layer was separated, dried over anhydrous sodium sulfate, and filtered off, and then the solvent was evaporated under reduced pressure. The residue was recrystallized from 95% ethanol to give compounds **1a** or **1b** as white crystalline solids.

N-(4-Acetylphenyl)-2-bromoacetamide (**1a**)^[30]

White crystals (94% yield); mp: 159–161°C (reported mp: 157°C).

N-(4-Acetylphenyl)-3-bromopropanamide (**1b**)^[21]

White crystals (93% yield); mp: 175–176°C, as reported.

4.1.3 | Synthesis of N-(4-acetylphenyl)-2-bromopropanamide (**1c**)

To a stirred solution of 2-bromopropionic acid (0.153 g, 1 mmol) in DCM (30 ml), triethylamine (0.152 g, 1.5 mmol) was added at 0–5°C. Ethyl chloroformate (0.119 g, 1.1 mmol) was then added slowly and stirring was continued at the same temperature for an additional 40 min. Then, 4-aminoacetophenone (0.135 g, 1 mmol) was added portion-wise and the mixture was stirred for an additional 12 hr at room temperature. The whole mixture was then transferred to a separating funnel, where it was washed successively with 5% NaHCO₃ (2 × 25 ml) and water (2 × 25 ml). The organic layer was separated, dried over anhydrous sodium sulfate, and filtered off, and then the solvent was evaporated under reduced pressure.^[23] The residue was crystallized from 95% ethanol to give compound **1c**. White crystals (90% yield); mp: 129–131°C. IR (KBr) ν (cm⁻¹): 3,275 (NH), 1,702 (NHCOCH₂), and 1,661 (COCH₃); ¹H-NMR (400 MHz, CDCl₃) δ ppm: 1.98 (3H, d, *J* = 7.6 Hz, CHCH₃), 2.59 (3H, s, COCH₃), 4.58 (1H, q, *J* = 7.6 Hz, CHCH₃), 7.67 (2H, d, *J* = 8.8 Hz, Ar-H), 7.97 (2H, d, *J* = 8.8 Hz, Ar-H), and 10.7 (1H, s, NHCO). MS (ESI) calcd for C₁₁H₁₃BrNO₂ [M + H]⁺: 270.01, found: 269.90.

4.1.4 | General procedure for the synthesis of ketone derivatives **2a–f**

To a stirred solution of the N-acyl-4-aminoacetophenone derivatives **1a–c** (1.1 mmol) in acetonitrile (10 ml), ciprofloxacin hydrochloride or norfloxacin was added (1 mmol). TEA (0.202 g, 2 mmol) was then added and the mixture was heated under reflux for 12–18 hr. The formed precipitate was filtered off while hot, washed with acetonitrile, and dried under vacuum to give compounds **2a–f**.^[21]

7-[4-[(4-Acetylphenylcarbamoyl)methyl]piperazin-1-yl]-1-cyclopropyl-6-fluoro-1,4-dihydro-4-oxoquinoline-3-carboxylic acid (**2a**)

White crystals (0.330 g, 62.5% yield); mp: 240–241°C; IR (KBr) ν (cm⁻¹): 3,258 (NH), 1,730 (carboxylic C=O), 1,693 (amidic C=O), 1,678 (COCH₃), and 1,625 (4-keto); ¹H-NMR (400 MHz, dimethyl sulfoxide [DMSO]-d₆) δ ppm: 1.15–1.23 (2H, m, cyclopropyl-H), 1.29–1.38 (2H, m, cyclopropyl-H), 2.53 (3H, s, COCH₃), 2.75–2.83 (4H, m, piperazinyl-H), 3.31 (2H, s, NHCOCH₂), 3.38–3.46 (4H, m, piperazinyl-H), 3.78–3.88 (1H, m, cyclopropyl-H), 7.57 (1H, d, *J*_{H-F} = 7.6 Hz, H8), 7.80 (2H, d, *J* = 8.8 Hz, Ar-H), 7.87 (1H, d, *J*_{H-F} = 13.6 Hz, H5), 7.94 (2H, d, *J* = 8.8 Hz, Ar-H), 8.65 (1H, s, H2), 10.14 (1H, s, NHCO), and 15.16 (1H, brs, COOH); ¹³C-NMR (100 MHz, DMSO-d₆) δ ppm: 8.04, 26.82, 36.30, 49.83, 52.75, 61.90, 106.75, 107.36, 111.46 (d, *J* = 23 Hz), 119.23, 129.79, 132.50, 139.71, 143.39, 145.56, 148.38, 152.25, 154.21, 166.32, 169.23, 176.85, and 196.90;

HRMS (ESI) calcd for C₂₇H₂₇FN₄O₅ [M-H]⁻: 505.1892, found: 505.1892.

7-[4-[2-(4-Acetylphenylcarbamoyl)ethyl]piperazin-1-yl]-1-cyclopropyl-6-fluoro-4-oxo-1, 4-dihydroquinoline-3-carboxylic acid (**2b**)

White powder (0.315 g, 61.4% yield); mp: 241–242°C; IR (KBr) ν (cm⁻¹): 3,273 (NH), 1,731 (carboxylic C=O), 1,674 (amidic C=O), 1,654 (COCH₃), and 1,616 (4-keto); ¹H-NMR (400 MHz, DMSO-d₆) δ ppm: 1.15–1.23 (2H, m, cyclopropyl-H), 1.29–1.38 (2H, m, cyclopropyl-H), 2.52 (3H, s, COCH₃), 2.59 (2H, t, *J* = 7.6 Hz, COCH₂CH₂N-), 2.65–2.73 (4H, m, piperazinyl-H), 2.78 (2H, t, *J* = 7.6 Hz, COCH₂CH₂N-), 3.32–3.40 (4H, m, piperazinyl-H), 3.77–3.87 (1H, m, cyclopropyl-H), 7.57 (1H, d, *J*_{H-F} = 7.6 Hz, H8), 7.73 (2H, d, *J* = 8.8 Hz, Ar-H), 7.90 (1H, d, *J*_{H-F} = 13.6 Hz, H5), 7.90 (2H, d, *J* = 8.8 Hz, Ar-H), 8.66 (1H, s, H2), 10.27 (1H, s, NHCO), and 15.09 (1H, s, COOH); ¹³C-NMR (100 MHz, DMSO-d₆) δ ppm: 8.02, 26.75, 34.81, 36.27, 49.96, 52.59, 53.92, 106.77, 107.38, 111.42 (d, *J* = 23 Hz), 118.85, 119.06, 129.84, 132.23, 139.70, 143.98, 145.66, 148.34, 153.49 (*J* = 248 Hz), 166.29, 171.14, 176.85, and 196.81; HRMS (ESI) calcd for C₂₈H₂₉FN₄O₅ [M-H]⁻: 519.2049, found: 519.2053.

7-[4-[1-(4-Acetylphenylcarbamoyl)ethyl]piperazin-1-yl]-1-cyclopropyl-6-fluoro-1,4-dihydro-4-oxoquinoline-3-carboxylic acid (**2c**)

Yellow powder (0.295 g, 57% yield); mp: 253–255°C; IR (KBr) ν (cm⁻¹): 3,280 (NH), 1,731 (carboxylic C=O), 1,691 (amidic C=O), 1,669 (COCH₃), and 1,623 (4-keto); ¹H-NMR (400 MHz, DMSO-d₆) δ ppm: 1.16–1.21 (2H, m, cyclopropyl-H), 1.28 (3H, d, *J* = 7.6 Hz, CHCH₃), 1.30–1.39 (2H, m, cyclopropyl-H), 2.53 (3H, s, COCH₃), 2.78–2.89 (4H, m, piperazinyl-H), 3.38–3.49 (5H, m, piperazinyl-4H + CHCH₃), 3.77–3.86 (1H, m, cyclopropyl-H), 7.57 (1H, d, *J*_{H-F} = 7.6 Hz, H8), 7.82 (2H, d, *J* = 8.8 Hz, Ar-H), 7.90 (1H, d, *J*_{H-F} = 7.6 Hz, H5), 7.94 (2H, d, *J* = 8.8 Hz, Ar-H), 8.66 (1H, s, H2), 10.08 (1H, s, NHCO), and 15.11 (1H, s, COOH); ¹³C-NMR (100 MHz, DMSO-d₆) δ ppm: 8.02, 12.83, 26.82, 36.28, 49.22, 50.17, 63.77, 106.72, 107.35, 111.43 (d, *J* = 23 Hz), 119.26, 119.74, 129.77, 132.48, 139.69, 143.49, 145.65, 148.35, 153.48 (d, *J* = 247 Hz), 166.30, 172.18, 176.84, and 196.89; HRMS (ESI) calcd for C₂₈H₂₉FN₄O₅ [M-H]⁻: 519.2049, found: 519.2053.

7-[4-[(4-Acetylphenylcarbamoyl)methyl]piperazin-1-yl]-1-ethyl-6-fluoro-1,4-dihydro-4-oxoquinoline-3-carboxylic acid (**2d**)

White crystals (0.250 g, 52.5% yield); mp: 261–262°C; ¹H-NMR (400 MHz, DMSO-d₆) δ ppm: 1.45 (3H, t, *J* = 7.6 Hz, NCH₂CH₃), 2.54 (3H, s, COCH₃), 2.76–2.84 (4H, m, piperazinyl-H), 3.31 (2H, s, NHCOCH₂), 3.40–3.48 (4H, m, piperazinyl-H), 4.58 (2H, q, *J* = 7.6 Hz, NCH₂CH₃), 7.20 (1H, d, *J*_{H-F} = 7.6 Hz, H8), 7.79 (2H, d, *J* = 8.8 Hz, Ar-H), 7.92 (1H, d, *J*_{H-F} = 13.6 Hz, H5), 7.94 (2H, d, *J* = 8.8 Hz, Ar-H), 8.92 (1H, s, Ar-H), 10.03 (1H, s, NHCO), and 15.25 (1H, s, COOH); ¹³C-NMR (100 MHz, DMSO-d₆) δ ppm: 14.77, 26.79, 49.50, 49.91, 52.79, 61.91, 106.19, 107.70, 111.70 (d, *J* = 23 Hz), 119.24, 119.74, 129.77,

132.54, 137.76, 143.37, 145.89 (d, $J = 10$ Hz), 148.84, 153.35 (d, $J = 248$ Hz), 166.47, 169.21, 176.66, and 196.87; HRMS (ESI) calcd for $C_{26}H_{27}FN_4O_5$ $[M-H]^-$: 493.1892, found: 493.1897.

7-[4-[2-(4-Acetylphenylcarbamoyl)ethyl] piperazin-1-yl]-1-ethyl-6-fluoro-4-oxo-1, 4-dihydroquinoline-3-carboxylic acid (**2e**)^[21]
White powder (0.270 g, 54% yield); mp: 275–276°C as reported.

7-[4-[1-(4-Acetylphenylcarbamoyl)ethyl]piperazin-1-yl]-1-ethyl-6-fluoro-1,4-dihydro-4-oxoquinoline-3-carboxylic acid (**2f**)
White powder (0.335 g, 68% yield); mp: 278–279°C; 1H -NMR (400 MHz, DMSO- d_6) δ ppm: 1.28 (3H, d, $J = 7.6$ Hz, $CHCH_3$), 1.44 (3H, t, $J = 7.6$ Hz NCH_2CH_3), 2.53 (3H, s, $COCH_3$), 2.74–2.84 (4H, m, piperazinyl-H), 3.38–3.44 (4H, m, piperazinyl-H), 3.46 (1H, q, $J = 7.6$, $CHCH_3$), 4.57 (2H, q, $J = 7.6$ Hz, NCH_2CH_3), 7.18 (1H, d, $J_{H-F} = 7.6$ Hz, H8), 7.80 (2H, d, $J = 8.8$ Hz, Ar-H), 7.91 (1H, d, $J_{H-F} = 13.6$ Hz, H5), 7.92 (2H, d, $J = 8.8$ Hz, Ar-H), 8.92 (1H, s, H2), 10.08 (1H, s, $NHCO$), and 15.23 (1H, s, $COOH$); ^{13}C -NMR (100 MHz, DMSO- d_6) δ ppm: 12.80, 14.75, 26.80, 49.25, 49.49, 50.29, 63.78, 106.18, 107.69, 111.68 (d, $J = 23$ Hz), 119.27, 119.70, 129.76, 132.51, 137.75, 143.48, 145.85, 148.84, and 153.35 (d, $J = 248$ Hz), 166.47, 172.18, 176.66, 196.87; HRMS (ESI) calcd for $C_{27}H_{29}FN_4O_5$ $[M-H]^-$: 507.2049, found: 507.2053.

4.1.5 | General procedure for the synthesis of oxime derivatives **3a–f** and **4a–f**

To a stirred mixture of the appropriate ketone **2a–f** (1 mmol) in absolute ethanol (10 ml) were added hydroxylamine hydrochloride or O-methyl hydroxylamine hydrochloride (3 mmol) and anhydrous sodium acetate (0.246 g, 3 mmol). The mixture was heated under reflux for 12–30 hr. The formed precipitate was filtered off while hot, washed with ethanol (2×5 ml), dried, and recrystallized from acetonitrile to give oximes **3a–f** or O-methyl oximes **4a–f**.^[22,25]

1-Cyclopropyl-6-fluoro-7-[4-(2-[(4-(1-(hydroxyimino)ethyl)phenyl)amino]-2-oxoethyl)piperazin-1-yl]-4-oxo-1,4-dihydroquinoline-3-carboxylic acid (**3a**)

White crystals (0.298 g, 55.8% yield); mp: 260–261°C; 1H -NMR (400 MHz, DMSO- d_6) δ ppm: 1.17–1.22 (2H, m, cyclopropyl-H), 1.30–1.37 (2H, m, cyclopropyl-H), 2.14 (3H, s, $CH_3C=NOH$), 2.77–2.84 (4H, m, piperazinyl-H), 3.27 (2H, s, $NHCOCH_2$), 3.40–3.50 (4H, m, piperazinyl-H), 3.80–3.88 (1H, m, cyclopropyl-H), 7.56–7.70 (5H, m, 4 Ar-H + H8), 7.90 (1H, d, $J_{H-F} = 13.6$ Hz, H5), 8.66 (1H, s, Ar-H), 9.78 (1H, s, $NHCO$), 10.93 (1H, s, $C=NOH$), and 15.09 (1H, s, $COOH$); ^{13}C -NMR (100 MHz, DMSO- d_6) δ ppm: 8.03, 11.81, 36.29, 49.85, 52.78, 61.91, 106.73, 107.35, 111.45 (d, $J = 23$ Hz), 119.68, 126.39, 129.78, 132.58, 139.41, 139.70, 145.61 (d, $J = 10$ Hz), 148.36, 152.91, 153.49 (d, $J = 248$ Hz), 166.32, 169.32, and 176.84; HRMS (ESI) calcd for $C_{27}H_{28}FN_5O_5$ $[M-H]$: 520.20017, found: 520.20056.

1-Cyclopropyl-6-fluoro-7-[4-[3-[(4-(1-(hydroxyimino)ethyl)phenyl)amino]-3-oxopropyl]piperazin-1-yl]-4-oxo-1,4-dihydroquinoline-3-carboxylic acid (**3b**)

White crystals (0.348 g, 63.4% yield); mp: 275–277°C; IR (KBr) ν (cm^{-1}): 1,699 (carboxylic $C=O$), 1,680 (amidic $C=O$), 1,628 (4-keto), and 1,601 ($C=N$), 1H -NMR (400 MHz, DMSO- d_6) δ ppm: 1.17–1.23 (2H, m, cyclopropyl-H), 1.29–1.35 (2H, m, cyclopropyl-H), 2.13 (3H, s, $CH_3C=NOH$), 2.56 (2H, t, $J = 7.6$ Hz, $COCH_2CH_2N$), 2.67–2.71 (4H, m, piperazinyl-H), 2.77 (2H, t, $J = 7.6$ Hz, $COCH_2CH_2N$), 3.35–3.45 (4H, m, piperazinyl-H), 3.80–3.84 (1H, m, cyclopropyl-H), 7.50–7.62 (5H, m, 4 Ar-H + H8), 7.90 (1H, d, $J_{H-F} = 13.6$ Hz, H5), 8.66 (1H, s, H2), 10.02 (1H, s, $NHCO$), 10.91 (1H, s, $C=NOH$), and 15.05 (1H, s, $COOH$); ^{13}C -NMR (100 MHz, DMSO- d_6) δ ppm: 8.02, 11.80, 34.69, 36.28, 49.95, 52.60, 54.06, 106.78, 107.34, 111.41 (d, $J = 23$ Hz), 119.27, 126.43, 129.87, 132.20, 139.69, 140.06, 145.57, 148.35, 152.91, 153.50 (d, $J = 249$ Hz), 166.32, 170.61, and 176.85; HRMS (ESI) calcd for $C_{28}H_{30}FN_5O_5$ $[M-H]$: 534.21582, found: 534.21643.

1-Cyclopropyl-6-fluoro-7-[4-[1-(4-(1-(hydroxyimino)ethyl)phenylamino)-1-oxopropan-2-yl]piperazin-1-yl]-4-oxo-1,4-dihydroquinoline-3-carboxylic acid (**3c**)

White crystals (0.309 g, 56.3% yield); mp: 255–257°C; 1H -NMR (400 MHz, DMSO- d_6) δ ppm: 1.16–1.21 (2H, m, cyclopropyl-H), 1.28 (3H, d, $J = 7.6$ Hz, $CHCH_3$), 1.30–1.35 (2H, m, cyclopropyl-H), 2.14 (3H, s, $COCH_3$), 2.78–2.86 (4H, m, piperazinyl-H), 3.40–3.47 (5H, m, piperazinyl-4H + $CHCH_3$), 3.80–3.84 (1H, m, cyclopropyl-H), 7.59–7.67 (5H, m, 4 Ar-H + H8), 7.89 (1H, d, $J_{H-F} = 13.6$, H5), 8.66 (1H, s, H2), 9.84 (1H, s, $NHCO$), 10.93 (1H, s, $C=NOH$), and 15.11 (1H, s, $COOH$); ^{13}C -NMR (100 MHz, DMSO- d_6) δ ppm: 8.02, 11.81, 12.98, 36.27, 49.27, 50.21, 63.75, 106.70, 107.38, 111.44 (d, $J = 23$ Hz), 119.72, 126.39, 129.75, 132.58, 139.51, 139.71, 145.66, 148.34, 152.94, 153.48 (d, $J = 247$ Hz), 166.31, 171.65, and 176.86; Anal. Calcd for $C_{28}H_{30}FN_5O_5$: C, 62.79; H, 5.65; N, 13.08. Found: C, 62.94; H, 5.71; N, 13.24.

1-Ethyl-6-fluoro-7-[4-[2-[(4-(1-(hydroxyimino)ethyl)phenyl)amino]-2-oxoethyl]piperazin-1-yl]-4-oxo-1,4-dihydroquinoline-3-carboxylic acid (**3d**)

White crystals (0.355 g, 68% yield); mp: 286–288°C; 1H -NMR (400 MHz, DMSO- d_6) δ ppm: 1.45 (3H, t, $J = 7.6$ Hz NCH_2CH_3), 2.14 (3H, s, $CH_3C=NOH$), 2.75–2.83 (4H, m, piperazinyl-H), 3.27 (2H, s, $NHCOCH_2N$), 3.42–3.48 (4H, m, piperazinyl-H), 4.59 (2H, q, $J = 7.6$ Hz, NCH_2CH_3), 7.20 (1H, d, $J_{H-F} = 7.6$ Hz, H8), 7.61 (2H, d, $J = 8.0$ Hz, Ar-H), 7.67 (2H, d, $J = 8.0$, Ar-H), 7.92 (1H, d, $J_{H-F} = 13.6$ Hz, H5), 8.92 (1H, s, H2), 9.78 (1H, s, $NHCO$), 10.94 (1H, s, $C=NOH$), and 15.26 (1H, s, $COOH$); ^{13}C -NMR (100 MHz, DMSO- d_6) δ ppm: 11.81, 14.77, 49.50, 49.93, 52.82, 61.92, 106.19, 107.70, 111.70 (d, $J = 23$ Hz), 119.27, 119.70, 126.40, 132.62, 137.76, 139.40, 145.95, 148.84, 152.92, 153.35 (d, $J = 248$ Hz), 166.48, 168.65, and 176.67; HRMS (ESI) calcd for $C_{26}H_{28}FN_5O_5$ $[M-H]$: 508.2001; found: 508.2005.

1-Ethyl-6-fluoro-7-[4-[3-((4-(1-(hydroxyimino)ethyl)phenyl)amino)-3-oxopropyl]piperazin-1-yl]-4-oxo-1,4-dihydroquinoline-3-carboxylic acid (**3e**)^[21]

White crystals; yield: (0.535 g, 65.8% yield); mp: 290–292°C as reported.

1-Ethyl-6-fluoro-7-[4-[1-(4-(1-(hydroxyimino)ethyl)phenylamino)-1-oxopropan-2-yl]piperazin-1-yl]-4-oxo-1,4-dihydroquinoline-3-carboxylic acid (**3f**)

White crystals (0.302 g, 56.2% yield); mp: 294–296°C; IR (KBr) ν (cm⁻¹): 3,266 (NH), 1,718 (carboxylic C=O), 1,678, (amidic), and 1,621 (4-keto C=O); ¹H-NMR (400 MHz, DMSO-*d*₆) δ ppm: 1.27 (3H, d, *J* = 7.6 Hz, CHCH₃), 1.43 (3H, t, *J* = 7.6 Hz, NCH₂CH₃), 2.14 (3H, s, CH₃C=NOH), 2.75–2.85 (4H, m, piperazinyl-H), 3.35–3.45 (4H, m, piperazinyl-H), 4.58 (2H, q, *J* = 7.6, NCH₂CH₃), 7.18 (1H, d, *J*_{H-F} = 7.6 Hz H8), 7.61–7.72 (4H, m, Ar-H), 7.91 (1H, d, *J*_{H-F} = 13.6 Hz, H5), 8.92 (1H, s, H2), 9.86 (1H, s, NHCO), 10.96 (1H, s, C=NOH), and 15.27 (1H, s, COOH); ¹³C-NMR (100 MHz, DMSO-*d*₆) δ ppm: 11.82, 13.00, 14.77, 49.28, 49.50, 50.29, 63.72, 106.19, 107.66, 111.68 (d, *J* = 23 Hz), 119.68, 126.39, 129.77, 132.54, 137.74, 139.51, 145.97, 148.86, 152.91, 153.3 (d, *J* = 248 Hz), 166.50, 171.63, and 176.66; HRMS (ESI) calcd for C₂₇H₃₀FN₅O₅ [M-H]⁻: 522.2158, found: 522.2161.

1-Cyclopropyl-6-fluoro-7-[4-[2-((4-(1-(methoxyimino)ethyl)phenyl)amino)-2-oxoethyl]piperazin-1-yl]-4-oxo-1,4-dihydroquinoline-3-carboxylic acid (**4a**)

White powder, yield (0.378 g, 71% yield); mp: 253–254 °C; ¹H-NMR (400 MHz, DMSO-*d*₆) δ ppm: 1.17–1.23 (2H, m, cyclopropyl-H), 1.32–1.38 (2H, m, cyclopropyl-H), 2.17 (3H, s, CH₃C=NOCH₃), 3.55–3.68 (8H, m, piperazinyl-H), 3.87 (2H, s, NHCOCH₂), 3.92 (3H, s, C=NOCH₃), 4.24 (1H, m, cyclopropyl-H), 7.63–7.68 (5H, m, 4 Ar-H + H8), 7.97 (1H, d, *J*_{H-F} = 13.6 Hz, H5), 8.70 (1H, s, H2), 9.78 (1H, s, NHCO), and 15.04 (1H, s, COOH); ¹³C-NMR (100 MHz, DMSO-*d*₆) δ ppm: 8.09, 12.56, 36.41, 46.94, 51.93, 57.53, 61.97, 107.39, 107.52, 111.73 (d, *J* = 23 Hz), 119.24, 119.82, 126.95, 132.12, 139.29, 139.61, 144.23, 148.58, 153.33 (d, *J* = 245 Hz), 153.94, 163.68, 166.22, and 176.90; Anal. Calcd for C₂₈H₃₀FN₅O₅: C, 62.79; H, 5.65; N, 13.08. Found: C, 62.98; H, 5.63; N, 13.37.

1-Cyclopropyl-6-fluoro-7-[4-[3-((4-(1-(methoxyimino)ethyl)phenyl)amino)-3-oxopropyl]piperazin-1-yl]-4-oxo-1,4-dihydroquinoline-3-carboxylic acid (**4b**)

White crystals (0.520 g, 95% yield); mp: 255–256°C; ¹H-NMR (400 MHz, DMSO-*d*₆) δ ppm: 1.19–1.23 (2H, m, cyclopropyl-H), 1.32–1.38 (2H, m, cyclopropyl-H), 2.07 (2H, t, *J* = 7.6 Hz, NHCOCH₂CH₂N), 2.16 (3H, s, CH₃C=NOH), 3.05 (2H, t, *J* = 7.6 Hz, NHCOCH₂CH₂N), 3.45–3.80 (8H, m, piperazinyl-H), 3.85–3.88 (1H, m, cyclopropyl-H), 3.91 (3H, s, C=NOCH₃), 7.60–7.69 (5H, m, 4 Ar-H + H8), 7.96 (1H, d, *J*_{H-F} = 13.6 Hz, H5), 8.69 (1H, s, H2), 10.42 (1H, s, NHCO), and 15.01 (1H, s, COOH); ¹³C-NMR (100 MHz, DMSO-*d*₆) δ ppm: 8.09, 12.54, 31.01, 36.40, 46.81, 51.28, 52.09, 61.92, 107.34, 107.54, 111.73 (d, *J* = 22 Hz), 119.48, 120.02, 126.82, 131.39,

139.60, 140.22, 144.20, 148.60, 153.34 (d, *J* = 248 Hz), 154.00, 166.19, 168.43, and 176.91; Anal. Calcd for C₂₉H₃₂FN₅O₅: C, 63.38; H, 5.87; N, 12.74. Found: C, 63.51; H, 5.90; N, 13.01.

1-Cyclopropyl-6-fluoro-7-[4-[1-(4-(1-(methoxyimino)ethyl)phenylamino)-1-oxopropan-2-yl]piperazin-1-yl]-4-oxo-1,4-dihydroquinoline-3-carboxylic acid (**4c**)

White crystals (0.290 g, 55.3% yield); mp: 242–244°C; ¹H-NMR (400 MHz, DMSO-*d*₆) δ ppm: 1.18–1.21 (2H, m, cyclopropyl-H), 1.32–1.38 (2H, m, cyclopropyl-H), 1.63 (3H, d, *J* = 7.6 Hz, CH₃CH), 2.17 (3H, s, CH₃C=NOCH₃), 3.58–3.84 (9H, m, piperazinyl-8H + 1H of CHCH₃), 3.91 (3H, s, C=NOCH₃), 4.32–4.36 (1H, m, cyclopropyl-H), 7.62–7.64 (1H, d, *J* = 7.6 Hz, H8), 7.64–7.76 (4H, m, Ar-H), 7.96 (1H, d, *J* = 13.6 Hz, H5), 8.69 (1H, s, H2), 10.99 (1H, s, NHCO), and 15.01 (1H, s, COOH); ¹³C-NMR (100 MHz, DMSO-*d*₆) δ ppm: 8.08, 12.57, 14.05, 36.39, 47.17, 49.46, 61.99, 63.54, 107.33, 107.54, 111.74 (*J* = 23 Hz), 119.58, 120.14, 126.89, 132.34, 139.21, 139.61, 144.24, 148.61, 153.59, 153.93, 166.20, 168.43, and 176.86; Anal. Calcd for C₂₉H₃₂FN₅O₅: C, 63.38; H, 5.87; N, 12.74. Found: C, 63.58; H, 5.94; N, 12.96.

1-Ethyl-6-fluoro-7-[4-[2-((4-(1-(methoxyimino)ethyl)phenyl)amino)-2-oxoethyl]piperazin-1-yl]-4-oxo-1,4-dihydroquinoline-3-carboxylic acid (**4d**)

White crystals (0.165 g, 65.22% yield); mp: 242–244 °C; ¹H-NMR (400 MHz, DMSO-*d*₆) δ ppm: 1.45 (3H, t, *J* = 7.6 Hz, NCH₂CH₃), 2.16 (3H, s, CH₃C=NOCH₃), 2.77–2.81 (4H, m, piperazinyl-H), 3.27 (2H, s, NHCOCH₂N), 3.40–3.46 (4H, m, piperazinyl-H), 3.91 (3H, s, C=NOCH₃), 4.59 (2H, q, *J* = 7.6 Hz, NCH₂CH₃), 7.20 (1H, d, *J*_{H-F} = 7.6 Hz, H8), 7.63–7.68 (4H, m, Ar-H), 7.92 (1H, d, *J*_{H-F} = 13.6 Hz, H5), 8.92 (1H, s, H2), 9.82 (1H, s, NHCO), and 15.26 (1H, s, COOH); ¹³C-NMR (100 MHz, DMSO-*d*₆) δ ppm: 12.56, 14.77, 49.50, 49.92, 52.08, 52.82, 61.92, 106.21, 107.70, 111.59 (d, *J* = 23 Hz), 119.68, 126.76, 131.41, 137.77, 139.93, 145.95, 148.85, 153.60 (d, *J* = 248 Hz), 154.02, 166.49, 168.75, and 176.68; Anal. Calcd for C₂₇H₃₀FN₅O₅: C, 61.94; H, 5.78; N, 13.38. Found: C, 62.23; H, 5.85; N, 13.61.

1-Ethyl-6-fluoro-7-[4-[3-((4-(1-(methoxyimino)ethyl)phenyl)amino)-3-oxopropyl]piperazin-1-yl]-4-oxo-1,4-dihydroquinoline-3-carboxylic acid (**4e**)

white crystals (0.404 g, 76% yield); mp: 278–279°C; ¹H-NMR (400 MHz, DMSO-*d*₆) δ ppm: 1.45 (3H, t, *J* = 7.6 Hz, NCH₂CH₃), 2.14 (3H, s, CH₃C=N-OH), 2.68 (2H, t, NHCOCH₂CH₂N) 2.75–2.84 (4H, m, piperazinyl-4H), 3.28 (2H, t, NHCOCH₂CH₂N) 3.40–3.48 (4H, m, piperazinyl-4H), 3.91 (3H, s, -C=NOCH₃), 4.59 (2H, q, *J* = 7.6 Hz, -N-CH₂CH₃), 7.19 (1H, d, *J*_{H-F} = 7.6 Hz s, H8), 7.62 (2H, d, *J* = 8.0 Hz, Ar-H), 7.66 (2H, d, *J* = 8 Hz, Ar-H), 7.91 (1H, d, *J*_{H-F} = 13.6 Hz, H5), 8.92 (1H, s, H2), 10.10 (1H, s, NHCO), and 15.25 (1H, s, -COOH); ¹³C-NMR (100 MHz, DMSO-*d*₆) δ ppm: 12.54, 14.77, 34.70, 49.50, 49.92, 52.81, 52.61, 61.90, 106.27, 107.70, 111.70 (d, *J* = 23 Hz), 119.70, 126.40, 132.63, 137.77, 139.40, 140.56, 145.94, 148.85, 153.36 (d, *J* = 248 Hz), 154.60, 166.48, 168.62, and 176.68; Anal.

Calcd for $C_{28}H_{32}FN_5O_5$: C, 62.56; H, 6.00; N, 13.03. Found: C, 62.78; H, 6.04; N, 13.39.

1-Ethyl-6-fluoro-7-[4-[1-(4-(1-(methoxyimino)ethyl)phenylamino)-1-oxopropan-2-yl]piperazin-1-yl]4-oxo-1,4-dihydroquinoline-3-carboxylic acid (**4f**)

White crystal (0.350 g, 66% yield); mp: 248–249°C; 1H -NMR (400 MHz, $DMSO-d_6$) δ ppm: 1.44 (3H, t, $J = 7.6$ Hz, $-NCH_2CH_3$), 1.58 (3H, d, $NCH(CH_3)CO$), 2.17 (3H, s, $CH_3C=NOCH_3$), 3.55–3.69 (9H, m, 8 piperazinyl-H + $CHCH_3$), 3.91 (3H, s, $CH_3C=NOCH_3$), 4.58 (2H, q, $-N-CH_2CH_3$), 7.26 (1H, d, $J_{H-F} = 7.6$, H8), 7.66 (2H, d, $J = 8.0$ Hz, Ar-H), 7.71 (2H, d, $J = 8.0$ Hz, Ar-H), 7.96 (1H, d, $J = 13.6$ Hz, H5), 8.95 (1H, s, H2), 10.42 (1H, s, $NHCO$), 15.27 (1H, s, $-COOH$); ^{13}C -NMR (100 MHz, $DMSO-d_6$) δ ppm: 12.57, 13.85, 14.83, 47.77, 49.41, 49.56, 61.97, 63.46, 106.79, 107.81, 111.91 ($J = 23$ Hz), 120.06, 120.40, 126.85, 132.17, 137.69, 139.36, 144.69, 149.04, 153.22 ($J = 248$ Hz), 153.94, 166.40, 171.69, and 176.66; Anal. Calcd for $C_{28}H_{32}FN_5O_5$: C, 62.56; H, 6.00; N, 13.03. Found: C, 62.85; H, 5.93; N, 13.25.

4.2 | Biological evaluation

4.2.1 | Screening of antimycobacterial activity

The antitubercular activity of the synthesized compounds, **2a–f**, **3a–f**, and **4a–f**, was evaluated using *M. tuberculosis* H37Rv strain via microplate Alamar blue assay (see Appendix A).

4.2.2 | Cleaved complex assay

Cleaved complex assay for compounds **2a**, **2b**, **3b**, **3c**, and ciprofloxacin have been evaluated, which include two main steps: purification of *M. tuberculosis* GyrA and GyrB proteins separately, followed by cleavage assay (see Appendix A).

4.2.3 | Screening of antibacterial activity

The antibacterial activity of compounds **2a–f**, **3a–f**, **4a–f**, norfloxacin, and ciprofloxacin against *S. aureus*, *E. coli* (ATCC 8739), *B. cereus* (AUMC No B-52), *M. luteus* (AUMC No B-112), *K. pneumonia* (AUMC No B-77), *P. aeruginosa* (AUMC No B-73), and *S. marcescens* (AUMC No B-54) was determined according to the standard agar cup diffusion method^[27,30] (see Appendix A).

4.3 | Docking study

The synthesized quinolone derivatives, **2b**, **2e**, **3b**, and **4b**, were docked into topoisomerase II (gyrase) to predict the possible binding interactions between these compounds and the enzyme active site.

Docking experiments were carried out using MOE 2014 software (see Appendix A).

ACKNOWLEDGMENTS

The authors thank Dr. Rehab M Abdel-Baky, Department of Microbiology and Immunology, Minia University, and Mycological Center (AUMC), Faculty of Science, Assiut University, Assiut, Egypt, for their great help in carrying out the antibacterial screening.

CONFLICTS OF INTERESTS

The authors declare that there are no conflicts of interests.

ORCID

Gamal El-Din A. Abuo-Rahma  <http://orcid.org/0000-0003-3908-1832>

REFERENCES

- [1] Global Tuberculosis Report 2019. Geneva, Switzerland, World Health Organization, <http://apps.who.int/iris> (accessed: 2020).
- [2] V. Šlachetová, M. Šebela, E. Torfs, L. Oorts, D. Cappoen, K. Berka, V. Bazgier, L. Brulíková, *Eur. J. Med. Chem.* **2020**, *185*, 111812.
- [3] N. Trotsko, J. Golus, P. Kazimierzczak, A. Paneth, A. Przekora, G. Ginalska, M. Wujec, *Bioorg. Chem.* **2020**, *97*, 103676.
- [4] J. Esteban, M. García-Coca, *Front. Microbiol.* **2018**, *8*, 2651.
- [5] T. Khan, K. Sankhe, V. Suvarna, A. Sherje, K. Patel, B. Dravyakar, *Biomed. Pharmacother.* **2018**, *103*, 923.
- [6] H. H. H. Mohammed, G. E.-D. A. Abuo-Rahma, S. H. Abbas, El-S. M. N. Abdelhafez, *Curr. Med. Chem.* **2019**, *26*, 1.
- [7] H. A. A. Ezelarab, S. H. Abbas, H. A. Hassan, G. E.-D. A. Abuo-Rahma, *Arch. Pharm. Chem. Life Sci.* **2018**, *351*, 1800141.
- [8] A. Aubry, X.-S. Pan, L. M. Fisher, V. Jarlier, E. Cambau, *Antimicrob. Agents Chemother.* **2004**, *48*, 1281.
- [9] T. Zhang, W. Shen, M. Liu, R. Zhang, M. Wang, L. Li, B. Wang, H. Guo, Y. Lu, *Eur. J. Med. Chem.* **2015**, *104*, 73.
- [10] Y.-Q. Hu, S. Zhang, F. Zhao, C. Gao, L.-S. Feng, Z.-Sh. Lv, Z. Xu, X. Wu, *Eur. J. Med. Chem.* **2017**, *133*, 255.
- [11] G. S. Timmins, S. Master, F. Rusnak, V. Deretic, *Antimicrob. Agents Chemother.* **2004**, *48*, 3006.
- [12] F. Rong, Y. Tang, T. Wang, T. Feng, J. Song, P. Li, W. Huang, *Antioxidants* **2019**, *8*, 556. <https://doi.org/10.3390/antiox8110556>
- [13] Z. Sadreiarhami, T.-K. Nguyen, R. Namivandi-Zangeneh, K. Jung, E. H. Wong, C. Boyer, *J. Mater. Chem. B* **2018**, *6*, 2945.
- [14] L. Yang, E. S. Feura, M. J. R. Ahonen, M. H. Schoenfish, *Adv. Healthc. Mater.* **2018**, *7*, 1800155. <https://doi.org/10.1002/adhm.201800155>
- [15] G. Fd-S. Fernandes, P. C. de Souza, L. B. Marino, K. Chegaev, S. Guglielmo, L. Lazzarato, R. Fruttero, M. C. Chung, F. R. Pavan, J. L. dosSantos, *Eur. J. Med. Chem.* **2016**, *123*, 523.
- [16] A. Wang, K. Lv, Z. Tao, J. Gu, L. Fu, M. Liu, B. Wan, S. G. Franzblau, C. Ma, X. Ma, B. Han, A. Wang, S. Xu, Y. Lu, *Eur. J. Med. Chem.* **2019**, *181*, 111595.
- [17] R. Ciccone, F. Mariani, A. Cavone, T. Persichini, G. Venturini, E. Ongini, V. Colizzi, M. Colasanti, *Antimicrob. Agents Chemother.* **2004**, *47*, 2299.
- [18] Y.-L. Fan, J.-B. Wu, X.-W. Cheng, F.-Z. Zhang, L.-S. Feng, *Eur. J. Med. Chem.* **2018**, *146*, 554.
- [19] J. Huang, M. Wang, B. Wang, Z. Wu, M. Liu, L. Feng, J. Zhang, X. Li, Y. Yang, Y. Lu, *Bioorg. Med. Chem. Lett.* **2016**, *26*, 2262.
- [20] H. A. Aziz, G. A. I. Moustafa, S. H. Abbas, G. Hauk, V. S. Krishna, D. Sriram, J. M. Berger, G. E.-D. A. Abuo-Rahma, *Med. Chem. Res.* **2019**, *28*, 1272.

- [21] H. A. Aziz, G. A. I. Moustafa, S. H. Abbas, S. M. Derayea, G. E.-D. A. A. AbuoRahma, *Eur. J. Chem.* **2017**, 8, 119. <https://doi.org/10.5155/eurjchem.8.2.119-124>
- [22] F. F. Ahmed, A. A. Abd El-Hafeez, S. A. Abbas, D. Abdelhamid D, M. Abdel-Aziz, *Eur. J. Med. Chem.* **2018**, 151, 705.
- [23] M. E. Shoman, M. Abdel-Aziz, O. M. Aly, H. H. Farag, M. A. Morsy, *Eur. J. Med. Chem.* **2009**, 44, 3068.
- [24] M. A. Mourad, M. Abdel-Aziz, G. E.-D. A. Abuo-Rahma, H. H. Farag, *Eur. J. Med. Chem.* **2012**, 54, 907.
- [25] K. Aldred, R. Kerns, N. Osherooff, *Biochem* **2014**, 53, 1565.
- [26] M. Harel, I. Schalk, L. Ehret-Sabatier, F. Bouet, M. Goeldner, C. Hirth, P. H. Axelsen, I. Silman, J. L. Sussman, *Proc. Natl. Acad. Sci. U. S. A.* **1993**, 90, 9031.
- [27] S. Gharaghani, T. Khayamian, M. Ebrahimi, *Environ. Res.* **2013**, 24, 773.
- [28] T. R. Blower, B. H. Williamson, R. J. Kerns, J. M. Berger, *Proc. Natl. Acad. Sci. U. S. A.* **2016**, 113, 1706.
- [29] B. Bonev, J. Hooper, J. Parisot, *J. Antimicrob. Chemother.* **2008**, 61, 1295.
- [30] H. Xie, D. Ng, S. N. Savinov, B. Dey, P. D. Kwong, R. Wyatt, A. B. Smith, W. A. Hendrickson, *J. Med. Chem.* **2007**, 50, 4898.

SUPPORTING INFORMATION

Additional supporting information may be found online in the Supporting Information section.

How to cite this article: Aziz HA, Moustafa GA, Abuo-Rahma GEDA, et al. Synthesis and antimicrobial evaluation of new nitric oxide-donating fluoroquinolone/oxime hybrids. *Arch Pharm.* 2020;e2000180.
<https://doi.org/10.1002/ardp.202000180>

APPENDIX A

BIOLOGICAL EVALUATION

Screening of antimycobacterial activity

The used strain is *M. tuberculosis* H37Rv strain. Briefly, the inoculum was prepared from the fresh LJ medium resuspended in the 7H9-S medium (7H9 broth, 0.1% casitone, 0.5% glycerol, supplemented oleic acid, albumin, dextrose, and catalase), adjusted to a McFarland tube No. 1, with 1:20 dilutions; 100 µl was used as inoculum. Each drug stock solution was thawed and diluted in 7H9-S at fourfold, the final highest concentration tested. Serial twofold dilutions of each drug were prepared directly in a sterile 96-well microtiter plate using 100 µl 7H9-S. A growth control containing no antibiotic and a sterile control were also prepared on each plate. Sterile water was added to all perimeter wells to avoid evaporation during the incubation. The plate was covered, sealed in plastic bags, and incubated at 37°C in a normal atmosphere. After 7 days of incubation, 30 µl of Alamar blue solution was added to each well, and the plate was reincubated overnight. A change in color from blue (oxidized state) to pink (reduced) indicated the growth of bacteria, and the MIC was defined as the lowest concentration of drug that prevented this change in color.

Cleaved complex assay

Protein purification

M. tuberculosis GyrA and GyrB proteins were purified separately, as described previously. Briefly, proteins were expressed from a pET28b derivative expression plasmid, producing a TEV-cleavable hexahistidine tag at the amino-terminus. Proteins were expressed in BL21 (DE3) *E. coli* cells containing the Rosetta 2 pLysS plasmid. Cells were grown to mid-log phase at 30°C and induced with 1-mM IPTG for 3 hr. Cells were then harvested by centrifugation and resuspended in A800 buffer (30-mM Tris-HCl, pH 7.8; 800-mM NaCl; 10-mM imidazole, pH 8.0; 10% glycerol; 0.5-mM TCEP; 1-µg/ml leupeptin; 1-µg/ml pepstatin; 1-mM PMSF). Cells were lysed by sonication and lysate was clarified by centrifugation. The soluble fraction was applied to 5-ml HisTrap HP columns and washed with 25 column volumes of A800. Captured His6-tagged GyrA or GyrB was eluted from the resin with B800 (30-mM Tris-HCl, pH 7.8; 800-mM NaCl; 500-mM imidazole, pH 8.0; 10% glycerol; 0.5-mM TCEP; 1-µg/ml leupeptin; 1-µg/ml pepstatin; 1-mM PMSF). Proteins were dialyzed separately against C500 buffer (30-mM Tris-HCl, pH 7.8; 500-mM NaCl; 10-mM imidazole; 10% glycerol; 0.25-mM TCEP) in the presence of His6-tagged TEV protease; uncleaved His6-tagged protein and TEV protease were removed by a second passage over a 5-ml HisTrap HP column. Cleaved proteins were concentrated and further purified by gel filtration over a sephacryl S-300HR column pre-equilibrated in A500 buffer (50-mM Tris, pH 7.8; 500-mM KCl; 10% glycerol; 0.5-mM TCEP). Fractions containing purified protein, as assessed by sodium dodecyl sulfate-polyacrylamide gel electrophoresis (SDS-PAGE), were collected and concentrated. For storage, concentrated protein was mixed, 1:1, with storage buffer (50-mM Tris, pH 7.8; 500-mM KCl; 50% glycerol; 0.5-mM TCEP), then flash-frozen as aliquots in liquid nitrogen, and stored at -80°C.

Cleavage assays

Fluoroquinolone compounds were resuspended in DMSO and stored at -80°C as 2.5–10 mM stocks. Purified *M. tuberculosis* GyrA and GyrB were combined, 1:1, to form the gyrase heterotetramer at a concentration of 40 µM; for assays, the holoenzyme was serially diluted in twofold steps to a final working concentration of 1.25 µM using gyrase dilution buffer (50-mM Tris, pH 7.8; 150-mM monopotassium glutamate; 5-mM MgOAc; 10% glycerol). Cleavage assays were prepared by mixing the following on ice: 4-µl 10× supercoiled plasmid DNA (125 nM); 4-µl 10× *M. tuberculosis* gyrase heterotetramer (1.25 µM); 10-µl 4× reaction buffer (120-mM Tris, pH 7.8; 38-mM MgOAc; 340-mM monopotassium glutamate; 36% glycerol; 0.4-mg/ml bovine serum albumin [BSA]; 4-mM TCEP); 20-µl distilled water; and 2-µl 20× fluoroquinolone compound dilutions. The final reaction conditions are as follows: 12.5-nM supercoiled DNA; 125-nM *M. tuberculosis* gyrase heterotetramer; 35-mM Tris, pH 7.8; 100-mM monopotassium glutamate; 10-mM MgOAc; 10% glycerol; 100-µg/ml BSA; and 1-mM TCEP; 0–500-µM fluoroquinolone compound. Cleavage reactions were conducted by incubating reactions at 37°C in the absence of ATP for 30 min. Reactions were stopped by the

addition of 2- μ l SDS (12%), followed immediately by the addition of 2- μ l 500-mM ethylenediaminetetraacetic acid. Stopped reactions were then mixed with 4- μ l proteinase K (3 mg/ml) and digested at 37°C for 25 min. Stopped and digested reaction products were then mixed with 10- μ l DNA loading dye, and products were resolved by running 20 μ l of the reaction dye mix on 1.5% TAE agarose gels with or without 1- μ g/ml ethidium bromide (EtBr). Gels were run at 35 V for 16.5 hr to resolve products and post-stained by soaking for 1 hr in 1- μ g/ml ethidium bromide, followed by 2 hr destaining in water. Gels were imaged by ultraviolet transillumination using a Gel Doc EZ gel imaging system (Bio-rad).

Screening of antibacterial activity

Microbial strains and culture conditions

The antibacterial activity of compounds **2a-f**, **3a-f**, **4a-f**, norfloxacin, and ciprofloxacin against *Staphylococcus aureus* and *Escherichia coli* was determined according to the standard agar cup diffusion method at Department of Microbiology, Faculty of Pharmacy, Minia University, Minia, Egypt. Standard strains of *S. aureus* and *Escherichia coli* (ATCC 8739) were obtained from the microbiological resource center, Faculty of Agriculture, Ain Shams University, Cairo, Egypt. Also, the antibacterial activity of compounds **2a-f**, **3a-f**, **4a-f**, norfloxacin, and ciprofloxacin against *Bacillus cereus* (AUMC No. B-52), *Micrococcus luteus* (AUMC No. B-112), *Klebsiella pneumonia* (AUMC No. B-77), *Pseudomonas aeruginosa* (AUMC No. B-73), and *Serratia marcescens* (AUMC No. B-54) was determined according to the standard agar cup diffusion method at Mycological Center (AUMC), Faculty of Science, Assiut University, Assiut, Egypt. All isolates were maintained at -70°C in trypticase soya broth (TSB; Becton and Dickinson) with 10% glycerol. Before inoculation, all isolates were subcultured at 37°C for 24 hr on trypticase soya agar (Becton and Dickinson) and TSB, respectively.

Determination of the minimum inhibitory concentration (MIC)

From all the tested bacteria, 0.5 ml of 1×10^8 CFU/ml (0.5 McFarland turbidity) were plated on sterile petri dishes, and then 20 ml of Mueller Hinton Agar media (Oxoid) were added to each petri dish.

The plates were rotated slowly to ensure uniform distribution of the microorganisms and then allowed to solidify on a flat surface. After solidification, four equidistant and circular wells of 10-mm diameter were carefully punched using a sterile cork bore. Twofold serial dilutions of the tested compounds using DMSO were performed. An equal volume of 100 μ l of each dilution was applied separately to each well in three replicates using a micropipette. All plates were incubated at 37°C for 24 hr. The inhibition zones were measured and their average was calculated. The MIC was calculated by plotting the natural logarithm of the concentration of each dilution of the tested compounds against the square of zones of inhibition and a regression line was drawn through the points, and then the antilogarithm of the intercept on the logarithm of concentration axis gave the MIC value.

Docking study

The synthesized Quinolone derivatives, **2b**, **2e**, **3b**, and **4b**, were docked on Topoisomerase II (gyrase) to predict the possible binding interactions between these compounds and the enzyme active site. Docking experiments were carried out using MOE 2014 software. Target compounds have been constructed into the builder interface of the MOE program; the energy was minimized until an RMSD (root mean square deviation) gradient of 0.01 Kcal/mol was achieved, and RMS distance of 0.1 Å with MMFF94X (Merck molecular force field 94x) force field and the partial charges were automatically calculated. The X-ray crystallographic structure of the ligand-enzyme complex was downloaded from protein data bank (www.rcsb.org); Topoisomerase II (gyrase) (PDB: 5bs8). The enzyme was prepared for the docking process by automatic protein correction and adding hydrogens to the 3D structure of the protein. Then, validation of the docking process was done by redocking of the cocrystallized ligand, and RMS distance with an MMFF94X force field, which was found to be 1.59 Å, and the partial charges were automatically calculated. Then, the designed compounds were docked instead. Docking was carried out with the default settings of MOE-DOCK. The obtained poses were studied and the poses that showed the best ligand-enzyme interactions were selected and stored for energy calculations.